ESC European Society of Cardiology

Cardiovascular Research (2023) **119**, 1427–1440
https://doi.org/10.1093/cvr/cvac116

A functional connectome signature of blood pressure in >30 000 participants from the UK biobank

Rongtao Jiang [1]*, Vince D. Calhoun[2], Stephanie Noble [1], Jing Sui[2], Qinghao Liang[3], Shile Qi[2], and Dustin Scheinost [1,3,4,5,6]*

[1]Department of Radiology and Biomedical Imaging, Yale School of Medicine, New Haven, CT 06510, USA; [2]Tri-institutional Center for Translational Research in Neuroimaging and Data Science (TReNDS), Georgia Institute of Technology, Emory University and Georgia State University, Atlanta, GA 30303, USA; [3]Department of Biomedical Engineering, Yale University, New Haven, CT 06520, USA; [4]Interdepartmental Neuroscience Program, Yale University, New Haven, CT 06520, USA; [5]Department of Statistics & Data Science, Yale University, New Haven, CT 06520, USA; and [6]Child Study Center, Yale School of Medicine, New Haven, CT 06510, USA

Received 26 April 2022; revised 7 June 2022; editorial decision 1 July 2022; online publish-ahead-of-print 25 July 2022

Aims

Elevated blood pressure (BP) is a prevalent modifiable risk factor for cardiovascular diseases and contributes to cognitive decline in late life. Despite the fact that functional changes may precede irreversible structural damage and emerge in an ongoing manner, studies have been predominantly informed by brain structure and group-level inferences. Here, we aim to delineate neurobiological correlates of BP at an individual level using machine learning and functional connectivity.

Methods and results

Based on whole-brain functional connectivity from the UK Biobank, we built a machine learning model to identify neural representations for individuals' past (~8.9 years before scanning, $N = 35\,882$), current ($N = 31\,367$), and future (~2.4 years follow-up, $N = 3\,138$) BP levels within a repeated cross-validation framework. We examined the impact of multiple potential covariates, as well as assessed these models' generalizability across various contexts.

The predictive models achieved significant correlations between predicted and actual systolic/diastolic BP and pulse pressure while controlling for multiple confounders. Predictions for participants not on antihypertensive medication were more accurate than for currently medicated patients. Moreover, the models demonstrated robust generalizability across contexts in terms of ethnicities, imaging centres, medication status, participant visits, gender, age, and body mass index. The identified connectivity patterns primarily involved the cerebellum, prefrontal, anterior insula, anterior cingulate cortex, supramarginal gyrus, and precuneus, which are key regions of the central autonomic network, and involved in cognition processing and susceptible to neurodegeneration in Alzheimer's disease. Results also showed more involvement of default mode and frontoparietal networks in predicting future BP levels and in medicated participants.

Conclusion

This study, based on the largest neuroimaging sample currently available and using machine learning, identifies brain signatures underlying BP, providing evidence for meaningful BP-associated neural representations in connectivity profiles.

* Corresponding authors. Tel: 203-824-2017, Email: dustin.scheinost@yale.edu (D.S.); Email: rongtao.jiang@yale.edu (R.J.)

Graphical Abstract

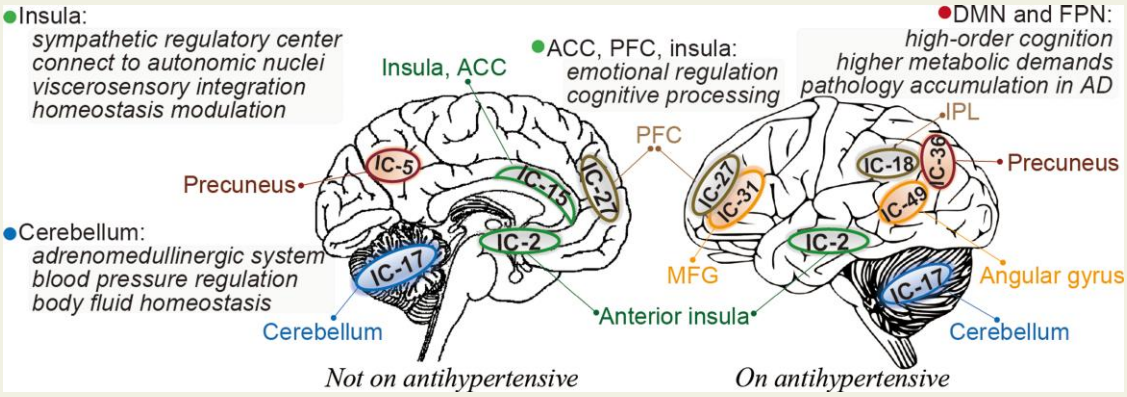

Keywords Predictive neuroimaging • Cardiovascular disease • Functional connectivity • Blood pressure • Hypertension

1. Introduction

Elevated blood pressure (BP) is a prevalent modifiable risk factor for cardiovascular diseases and a leading contributor to morbidity and mortality worldwide.[1] The pathophysiology of hypertension is intricate, spanning a wide variety of genetic factors and lifestyle, environmental, and health-related exposures.[2] Cumulative evidence suggests that midlife hypertension can exert a cascade of deleterious effects on brain structure and function, which can manifest later in life as cognitive impairment, dementia, and Alzheimer's disease (AD).[3,4] Thus, better understanding the neurobiological underpinnings of elevated BP may hold promise in revealing brain targets for early interventions.

Several studies have established the link between elevated BP and changes in brain structure.[5] Specifically, white matter hyperintensities, alongside microscale grey and white matter atrophy,[6–8] are established hallmarks of hypertension. Nevertheless, the emergence of these macroscopic signs of brain damage frequently signifies a final stage of widespread structural degeneration, which is considered irreversible.[9] Accordingly, antihypertensive therapies fail to reverse cognitive decline and protect the brain from microstructural damage, putatively since BP has progressed to clinical levels.[4] Further, a recent UK Biobank study of over 30 000 subjects reveals that white matter hyperintensities are more strongly associated with previous than concurrent BP, especially before the age of 50, implying the subtle, early changes associated with elevated BP may be undetectable from brain structure.[7] Furthermore, another study observes that the past rather than the current vascular risk factor burden is most strongly associated with lower brain volume.[10] Evidence from recent studies indicates that changes in brain function likely precede any irreversible structural damage.[11–13] In this regard, functional neuroimaging data, such as functional connectivity—or the temporal statistical dependencies between neural activity across spatially distinct but functionally coherent brain regions—may be better at detecting these subtle brain correlates of elevated BP. For example, Thaddeus *et al.* found that mean cerebrovascular reactivity was significantly reduced in the default mode network for subjects with pre-hypertension/hypertension and suggested that this functional measurement can serve as a preclinical marker for brain dysfunction in later life.[14] Another study suggests that the reduced hippocampal connectivity was associated in a graded way with increased BP and mediated the association between hypertension history and impaired memory in 19 507 participants from the UK biobank.[15] In this sense, a primary aim of this study is to examine the neuroimaging correlates of BP utilizing functional connectivity.

Increasing in popularity to analyze neuroimaging data, machine learning is a powerful means to dissect individual differences in whole-brain functional connectivity profiles, known as a connectome.[16,17] Such data-driven analyses have catalyzed neuroimaging research shifting from group-level inferences towards individual-level characterizations,[18–20] allowing for the investigation of brain correlates across the entire BP spectrum.[21] However, neural signatures of systolic BP (SBP)/diastolic BP (DBP) and pulse pressure (PP) are lacking, impeding efforts to pinpoint robust early changes in brain function associated with BP. Therefore, our second aim is to identify a connectome-based brain signature that is predictive of BP at the individual level, and test to what extent the signature can generalize across different contexts, especially between participants on or off antihypertensives.

To this end, we leveraged the UK Biobank, which provides a very large sample of neuroimaging data as well as cardiovascular risk factors,[22,23] to identify BP-associated brain changes in functional connectivity using machine learning. First, using partial least squares regression (PLSR), we define a neural signature predictive of novel individuals' past (mean 8.91 years before scanning, $N = 35\,882$), concurrent ($N = 31\,367$), and future (mean 2.40 years follow-up, $N = 3\,138$) BP levels separately within a repeated cross-validation framework. We examined the impact of multiple potential covariates, as well as assess these models' generalizability across various ethnic/racial groups. Second, we extracted the most predictive brain patterns from each model, quantified their similarities, and identified brain regions contributing differently to prediction across the three time points. Finally, we compared the brain signatures of participants based on medication status. Based on currently available evidence, our hypothesis is twofold. First, we hypothesize that we can identify a generalizable brain signature using functional connectivity that is predictive of individuals' BP levels. Our second hypothesis is that the predictive connectivity patterns may primarily involve brain regions associated with

high-order cognitive processing,[24] AD-related pathologies,[25] and central autonomic network.[26]

2. Methods

2.1 Cohort and participants

The UK Biobank project is an ongoing large-scale, longitudinal cohort study of participants recruited from across the UK. Between 2006 and 2010, baseline data was collected including deep genetic and a rich variety of phenotypic and health-related information (including lifestyle indicators, cognitive tests, physical measures, and biomarkers in blood and urine, but not brain imaging scans) from over half a million participants aged 40∼69 years from 22 dedicated centres (the 'baseline assessment visit').[23] Since 2014, a subsample of participants has been invited back to four assessment centres for brain imaging scanning (the 'first imaging visit'). Another follow-up imaging session started in 2019 (the 'repeat imaging visit'). BP readings were taken during each of the three visits.

The studies adhered to the Declaration of Helsinki. Written informed consent was obtained from all participants, and the study was approved by the North West Multicenter Research Ethics Committee (No. 11/NW/0382). This research was conducted using the UK Biobank resource under application number34 175.

We selected participants based on the availability of usable resting-state fMRI and BP data. Additional exclusion criteria included excessive head motion [defined as a mean framewise displacement (FD)>0.25 mm], and self-reported non-white racial background (see supplementary material online, *Figure S1*). In total, the current study comprised a sample of 35 882, 31 367, and 3 138 participants for the baseline assessment visit, the first imaging visit, and the repeated imaging visit, respectively (*Figure 1A*). The time intervals between the first two and last two visits were 8.91 ± 1.79 years (median = 9 years) and 2.40 ± 0.85 years (median = 2 years) respectively. Broadly, at the first imaging visit, participants were 53.42% females, aged 63.94 ± 7.65 years (range: 45∼82), and had a mean education of 13.78 ± 4.33 years (see supplementary material online, *Table S1*). *Table 1* summarizes the demographic characteristics of participants from three visits relevant to this study.

2.2 BP measurement

After the participant had been at rest for at least 5 min in the seated position, BP was collected twice, moments apart, by trained nurses using an Omron digital HEM-705IT monitor automatedly (taken using the left upper arm only unless this was not practical). The two sets of measurements demonstrated high test-retest reliability for all three data visits (intra-class correlation ranged from 0.83 to 0.87, see Supplementary material online, *Figure S2*). SBP and DBP were derived as the average across the two readings, or as a single reading if only one was available (Fields ID: 4079, 4080). PP was calculated as the difference between mean SBP and DBP. BP levels between different data visits were significantly correlated (range: 0.53–0.68, see Supplementary material online, *Figure S3*).

2.3 Data acquisition and preprocessing

Resting-state fMRI data were acquired in 3T Siemens Skyra scanners from each imaging centre using a standard 32-channel head coil (see Supplementary material online). The whole-brain functional connectomes used in this study were derived from the image-derived phenotypes, which were preprocessed, quality controlled, and made publicly available by the UK Biobank imaging team. An extensive overview of the data acquisition protocols and preprocessing carried out on behalf of UK Biobank can be found in https://biobank.ctsu.ox.ac.uk/crystal/crystal/docs/brain_mri.pdf and elsewhere.[22,28]

Data preprocessing, group independent component analysis (ICA) parcellation, and connectivity estimation were carried out using FSL. Briefly, this included motion correction using MCFLIRT, grand mean intensity normalization, high-pass temporal filtering, echo-planar image unwarping, gradient distortion correction unwarping, and removal of structured artefacts via ICA + FIX (16). Based on the preprocessed fMRI data, group ICA using FSL's MELODIC was performed to estimate 100 components that can be considered as 'parcellations' of cortical and subcortical grey matter. Forty-five ICA components that were clearly identifiable as artefactual were discarded, leaving 55 components for network modelling (*Figure 1B*; see Supplementary material online, *Figure S4*). The set of ICA spatial maps was mapped onto each subject's rs-fMRI time-series using dual-regression to derive subject-specific representative time-series per component (each component can be seen as a network 'node').[28]

Finally, partial correlations were estimated between time-series across 490 time points for each possible pair of nodes using FSLNets (http://fsl.fmrib.ox.ac.uk/fsl/fslwiki/FSLNets), resulting in a 55× 55 symmetric network matrices for each subject. Network matrix values were L2 regularized and normalized by Fisher's r-to-z transformation, as described in.[27,29] Overall, these connectomes consist of 1485 unique connections (edges) for further analyses.

2.4 Developing connectome-based signatures of SBP and DBP

Within a 10-fold cross-validation framework, we implemented a data-driven, machine learning approach to predict individuals' past, concurrent, and future BP levels separately based on whole-brain connectomes. The dataset was randomly split into 10 non-overlapping subsets. We first characterized the relationship between connectivity patterns and BP levels based on 9-fold training data using PLSR.[30] The PLSR has a good resilience to multicollinearity data (as it transforms high-dimensional features into a compact set of latent variables) and has been widely used for predicting multiple phenotypic measures.[31–33] Second, we calculated the predicted BP values for the left-out fold testing data using the dot product of the learned weight map with vectorized connectome strength. By designating each fold data as the testing set once, we can derive the predicted BP for all participants. To account for the influence of data split, we repeated the entire process 200 times on randomly partitioned data.[32,34].

Model performance was quantified as the mean Pearson's correlation (r) between model-predicted and actual BP levels, cross-validation R^2, and root mean squared error (RMSE), averaged across 200 repetitions. We employed a permutation test to determine the significance of the prediction correlation, by first randomly shuffling the BP values 10 000 times and then rerunning the prediction analysis, generating a null distribution of r values.[18] The P-value was determined by calculating the frequency with which the true model's r value exceeds the permutation-derived r values.[31]

2.5 Examining the influence of potential confounds on prediction

Multiple factors are hypothesized to be associated with SBP/DBP/PP.[35,36] To determine whether our models are robust to potential

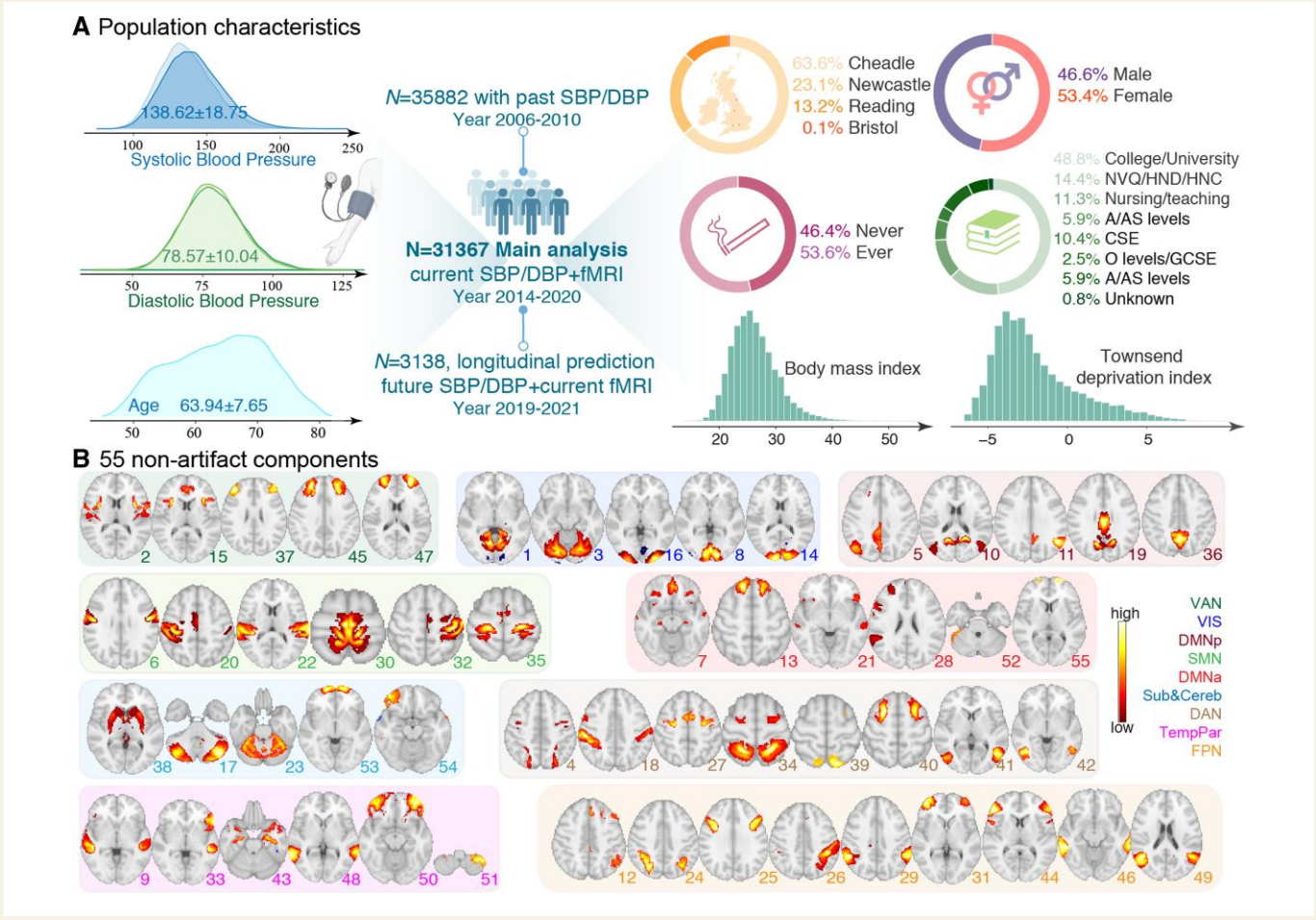

Figure 1 Population characteristics and the ICA-derived 55 components in the UK Biobank cohort. (*A*) The current study includes a respective of 35 882, 31 367, and 3 138 participants for the initial assessment visit, the first imaging visit, and the repeated imaging visit from the UK Biobank. (*B*) Each of the 55 non-artificial group-level components generated from group ICA were visualized in axial views and grouped into nine typical large functional networks.[27] DMNa, default mode network anterior; DMNp, default mode network posterior; SMN, somatomotor network; Sub&Cereb, subcortical and cerebellar network; TempPar, temporoparietal network; VAN, ventral attention network; VIS, visual network.

confounds and which factor impacts the prediction most, we controlled for the following covariates in the prediction: age, gender, body mass index (BMI), imaging acquisition centres, education attainment, smoking status (ever vs. never), socioeconomic status (measured by the Townsend Deprivation Index), and head motion.

To further control for head motion, we identified a subset of participants with a liberal (FD < 0.5 mm, N = 32 459) or a stringent threshold (FD < 0.15 mm, N = 25 179), and then reran the cross-validated prediction procedure 200 times.

2.6 Generalizing models across different contexts

Having established the neurophysiological plausibility of the BP-predictive models, we then turned to examine their generalizability across different contexts. We first tested the model's sensitivity to heterogeneity in imaging acquisition sites by implementing a leave-one-site-out cross-validation, where data from one of the four sites served as the testing set and data from the other three sites served as the training set.[37]

Since our main prediction was performed on participants of white origin, we next examined whether the brain signature can generalize to non-White populations. We defined the predictive models on the full set of White participants and then applied them directly to 1003 non-White validation samples. Finally, we tested whether our models can generalize to predict BP scores for participants whose fMRI data were independently collected from the repeat imaging visit. Rather than defining the brain signatures on the full set of 31 367 participants, we restricted model building to participants who only have fMRI data in the first imaging visit ($N = 29\,453$) and tested on participants who have fMRI data in the repeated imaging visit ($N = 2554$).

2.7 Determining the functional neuroanatomical basis of the brain signatures and comparing weight patterns among different models

Since our approach was implemented within a 10-fold cross-validation framework with 200 repetitions, 2000 different models were built in total, for which the weight pattern of the brain signatures can differ slightly from fold to fold.[38,39] To characterize the neurobiological basis of the brain signatures, we averaged feature weights across all 2000 models, yielding a connectivity-level weight map with larger absolute values indicating greater contributions to prediction.[34,38] To facilitate the

Table 1 Demographic information of participants relevant to this study

Variable	Baseline assessment visit	First imaging visit	Repeated imaging visit
N	35 882	31 367	3138
Age	55.05 ± 7.51	63.94 ± 7.65	64.63 ± 7.23
(mean ± SD, range)	40~70	45~82	50~82
Sex, N/%			
Female	19 221/53.57	16 756/53.42	1650/52.58
Male	16 661/46.43	14 611/46.58	1488/47.42
SBP (mmHg, mean ± SD)	134.82 ± 17.75	138.62 ± 18.75	140.89 ± 18.64
DBP (mmHg, mean ± SD)	81.20 ± 9.87	78.57 ± 10.04	79.40 ± 9.95
BMI (kg/m^2, mean ± sd)	26.33 ± 4.01	26.25 ± 4.10	26.28 ± 4.09
Socioeconomic status (mean ± SD)	−1.94 ± 2.68	−1.99 ± 2.66	−2.08 ± 2.60
Data acquisition date	03/16/2006	05/08/2014	05/22/2019
(range)	10/01/2010	03/13/2020	04/25/2021
FD (*mm*, mean ± SD)	0.12 ± 0.04	0.12 ± 0.04	0.11 ± 0.04
Imaging centres, N/%			
Cheadle	21 742/60.59	19 958/63.63	1788/56.98
Reading	5698/15.88	4125/13.15	90/2.87
Newcastle	8392/23.39	7244/23.09	1260/40.15
Bristol	50/0.14	40/0.13	0/0
Smoking status, N/%			
Never	14 778/42.94	13 998/46.45	1436/47.49
Ever	19 639/57.06	16 137/53.55	1588/52.51
Education levels, N/%			
College/University	16 630/46.35	15 297/48.77	1519/48.41
A/AS levels	2080/5.80	1848/5.89	193/6.15
O/GCSE levels	3837/10.69	3276/10.44	348/11.09
CSEs	930/2.59	788/2.51	95/3.03
NVQ/HND/HNC	5367/14.96	4505/14.36	480/15.30
Nursing/teaching	4492/12.52	3536/11.27	319/10.17
None of the above	2207/6.15	1867/5.97	166/5.29
Unknown	339/0.94	250/0.80	18/0.57

AS, Advanced Subsidiary; CSE, Certificate of Secondary Education; GCSE, General Certificate of Secondary Education; HNC, Higher National Certificate; HND, Higher National Diploma; NVQ, National Vocational Qualification.

interpretation of the predictive model, we further summarized these connectivity-level weight maps to component-wise representations. Specifically, we characterized a component's importance in prediction by adding up the absolute weight averages of its 54 connected edges.

We next quantified the similarity of weight patterns across different models. Specifically, we examined the edgewise and component-wise correlations of weight maps between SBP and DBP, as well as between different time points.[20] Significance of correlations was assessed by permuting the weight maps 10 000 times. Based on components having the top 10% ($N = 6$) absolute contribution weights, we further ascertained which components consistently had high predictive power for SBP, DBP or PP across all three time points, as well as which components uniquely had high predictive power for SBP/DBP/PP at one time point but not for the other two.

2.8 Comparing brain signatures of participants on or off antihypertensive medication

At the time of the first imaging visit, 6499 participants reported taking antihypertensives, while 22 642 participants reported not. To investigate whether brain connectivity can predict BP values for participants taking antihypertensives and whether their brain signatures differed from those not on antihypertensive treatment, we separately built a predictive model for each group using PLSR and evaluated its performance within a repeated cross-validation framework. Additionally, we evaluated the similarity of predictive brain patterns at the connectivity and component levels and examined which brain regions, among the most predictive ones, contributed differently between these two groups.

3. Results

3.1 Connectome-based signatures of BP across different time points

Within a machine learning framework, we separately identified a whole-brain, connectome-based signature that was predictive of individuals' past, concurrent, and future SBP/DBP/PP using ICA-derived functional network connectivity. As expected, significant correlations between predicted and actual BP levels were observed (*Figure 2A*; see Supplementary material online, *Figure S5 and Table S2*). Specifically, the highest prediction accuracy was achieved for current SBP, with a mean correlation reaching $r = 0.445 \pm 0.0007$ (cross-validation $R^2 = 19.6\%$, RMSE = 16.81 ± 0.0072), averaged across 200 cross-validation

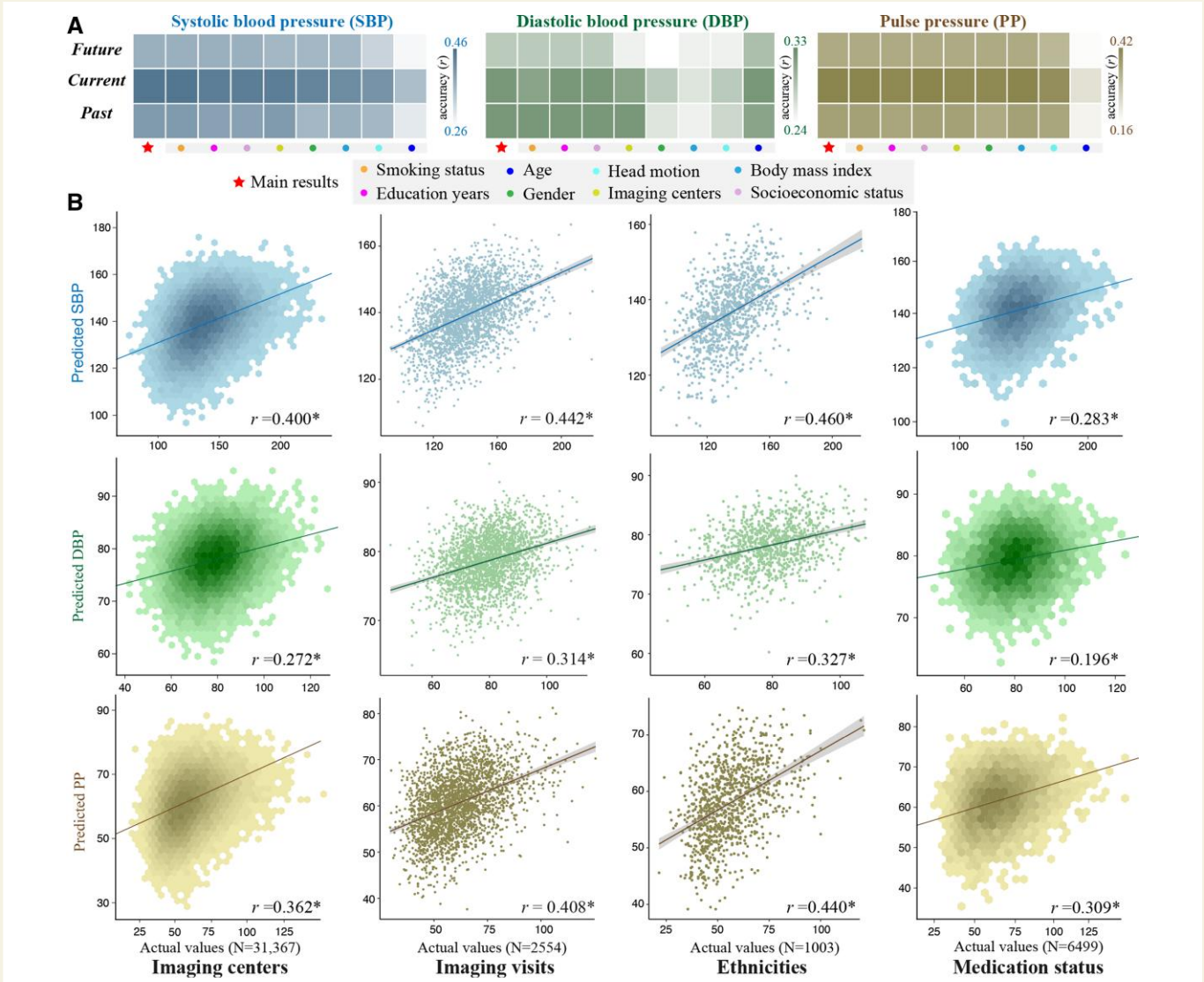

Figure 2 Patterns of whole-brain connectivity predicted BP levels and generalized across contexts. (*A*) Within a repeated cross-validation framework, connectome-based machine learning models successfully predicted past, current, and future BP levels, and prediction correlations remained significant after adjusting for a set of covariates including age, gender, education attainment, socioeconomic status, smoking history, imaging centres, and FD. Darker cell colors indicate higher predictive accuracy. (*B*) Predictive models showed strong generalizability across different contexts in terms of ethnicities (from whites to non-whites), data acquisition sites ($n = 4$), imaging visits (from the first imaging visit to the repeated imaging visit of UK Biobank cohort), and medication status (from unmedicated participants to those taking antihypertensives).

repetitions. The prediction performance was slightly attenuated for previous ($r = 0.398 \pm 0.0008$, $R^2 = 15.5\%$, RMSE = 16.34 ± 0.0068) and future SBP ($r = 0.374 \pm 0.003$, $R^2 = 11.9\%$, RMSE= 17.49 ± 0.033). For DBP, the brain signature achieved comparable prediction accuracies for previous ($r = 0.317 \pm 0.0009$, $R^2 = 9.6\%$, RMSE = 9.41 ± 0.0038) and current ($r = 0.315 \pm 0.0009$, $R^2 = 9.4\%$, RMSE= 9.55 ± 0.0038) measures, followed by a slightly lower accuracy for future measure ($r = 0.282 \pm 0.004$, $R^2 = 4.2\%$, RMSE= 9.74 ± 0.019). The prediction accuracies were $r = 0.359 \pm 0.0007$ ($R^2 = 12.6\%$, RMSE = 11.61 ± 0.0040), $r = 0.418 \pm 0.0009$ ($R^2 = 17.3\%$, RMSE = 13.37 ± 0.0051), and $r = 0.344 \pm 0.0036$ ($R^2 = 9.1\%$, RMSE= 13.86 ± 0.028) for previous, current and future PP, respectively. All predictions were statistically significant at $P < 10^{-4}$ under permutation tests (see Supplementary material online, *Figure S6*). Prediction using an alternative machine learning approach (connectome-based predictive modelling) was also significant albeit with a lower accuracy (see Supplementary material online, *Figure S7*). In comparison, when building models using connectivity data from the repeated imaging visit, we observed reduced prediction accuracies compared, which can be attributed to a largely reduced sample size (see Supplementary material online, *Figure S8*).

3.2 Influence of potential confounds on model performance

After controlling for a set of covariates, the prediction correlations remained significant ($P < 10^{-4}$, Bonferroni corrected, Table S2), suggesting robustness of the predictive models to these confounds (*Figure 2A*). Among all confounding variables, age exerted the greatest impact on

the prediction of SBP and PP but minimal impact on DBP, hinting at the possibility that SBP and DBP may follow distinct aging trajectories. In comparison, the most significant factor affecting DBP was BMI.

When restricting prediction analyses to only subjects with either a liberal or conservative head motion threshold, we observed nearly identical results in terms of prediction accuracies and the weight profile (correlations between weight patterns $r > 0.96$, $P < 10^{-4}$; see Supplementary material online, *Figure S9*).

3.3 Models are generalizable across contexts

When running the prediction procedure using a leave-one-site-out cross-validation, we observed significant correlations between predicted and actual values (r[SBP] = 0.400, r[DBP] = 0.272, r[PP] = 0.362, $P < 10^{-4}$, *Figure 2B*). Likewise, models defined on the full set of 31 367 participants of European White ancestry successfully generalized to 1003 non-Whites (r[SBP] = 0.460, r[DBP] = 0.327, r[PP] = 0.408, $P < 10^{-4}$). Furthermore, these models also predicted BP values for 2554 participants whose fMRI data were independently acquired from the UK Biobank's repeated imaging visit (r[SBP] = 0.442, r[DBP] = 0.314, r[PP] = 0.440, $P < 10^{-4}$). Moreover, the models also showed strong generalizability across gender, age, and BMI (see Supplementary material online, *Figure S10*). Taken together, these results provide evidence for the generalizability of the connectome-based brain signatures.

3.4 Functional neuroanatomical basis of the predictive brain signatures and the overlap

Figure 3 depicts the raw predictive weights averaged across all 200 cross-validation loops for previous, present, and future SBP/DBP. Considering the high similarity of weight maps between SBP and PP, we only show the predictive brain signatures for SBP here, and detailed results for PP can be found in Supplementary material online, *Figure S11*. Notably, weight maps across 2000 models demonstrated remarkably high correlations with each other, evidencing the stability of the brain signatures (see Supplementary material online, *Figure S12*). To aid in characterization, we demonstrate the top 60 connections according to their magnitude of contributing weights. The most predictive patterns were prominent in connections among cerebellar network, frontoparietal network (FPN), dorsal attention network (DAN) and ventral attention networks, and posterior default mode network. Among the top 60 edges, the SBP-current model shared 61.67% connections with the SBP-past model, and 31.67% connections with the SBP-future model while, the DBP-current model had 41.67 and 20% connections in common with DBP-past and DBP-future models ($P < 10^{-4}$, determined using the hypergeometric cumulative function).

As expected, predictive models of SBP and DBP demonstrated a high degree of edge-level similarity at each time point ($r = 0.640$–0.679, $P < 10^{-4}$ via permutation test; see Supplementary material online, *Figure S13*). The brain signature of current BP was also highly correlated with that of previous and future BP ($r = 0.474$–0.794, $P < 10^{-4}$).

Figure 4A shows component-level representations of mean absolute weights for all 6 models (SBP and DBP across 3 times). Results of separately summing the positive and negative predictive weights for each component can be found in Supplementary material online, *Figure S14*. In line with connectivity-wise similarities between these models, we observed even stronger correlations ($r = 0.507$–0.850, $P < 10^{-4}$; see Supplementary material online, *Figure 4C*). Further, the top 6 most predictive components were also highly overlapped (*Figure 4B*; see Supplementary material online, *Table S3*). Specifically, IC-17 (cerebellum), IC-2 (anterior insula and supramarginal gyrus), IC-27 (precentral gyrus and dorsolateral prefrontal cortex), and IC-15 [insula and anterior cingulate cortex (ACC)] were congruently highly predictive of SBP at all three time points (*Figure 4C*). In contrast, IC-36 (precuneus), IC-18 (inferior parietal and postcentral gyrus), and IC-39 (precuneus and superior parietal gyrus) demonstrated high predictive power for future SBP but not current SBP. IC-38 (putamen and caudate) and IC-23 (cerebellum and vermis) showed greater contributions to past SBP than current SBP. For DBP, IC-17 also emerged as the most predictive component. IC-23 (cerebellum vermis) and IC-2 had a greater predictive ability for previous and current DBP than for future DBP, whereas IC-15 and IC-25 (inferior frontal gyrus) had a greater predictive ability for previous DBP. IC-36 and IC-49 (angular gyrus) showed prominent contributions to predict future DBP but not for current or previous DBP.

3.5 Influence of taking antihypertensives on prediction

Overall, the repeated cross-validation in individuals taking antihypertensive medication generated significant predictions, but at a lower accuracy than models built on the entire sample. Notably, predictions for participants not on antihypertensive medication (r[SBP]= 0.441 ± 0.0009, RMSE[SBP] = 16.52 ± 0.0091; r[DBP] = 0.324 ± 0.0012, RMSE[DBP] = 9.48 ± 0.0054, $P < 10^{-4}$) were more accurate than predictions for currently medicated participants (r[SBP] = 0.243 ± 0.0027, RMSE[SBP]= 17.46 ± 0.0202; r[DBP] = 0.186 ± 0.0041, RMSE[DBP] = 10.01 ± 0.0169; $P < 10^{-4}$). After controlling for a set of covariates, the prediction correlations remained significant (see Supplementary material online, *Table S4*). Moreover, the predictive models showed comparable accuracies across different antihypertensive medications (*Figure 5A*), and models defined on unmedicated participants also generalized to participants taking antihypertensives (*Figure 2B*). When adjusting BP values by adding 15 and 10 mm Hg to SBP and DBP, respectively, for individuals reported to be taking antihypertensive medication, we observed nearly unchanged results in terms of the prediction accuracies and the predictive features (see Supplementary material online, *Figure S15*).

The brain weight maps from participants not on antihypertensives showed a high degree of correlation with those defined on the full sample, implying that including these subjects has only a weak influence on the identified brain signatures (see Supplementary material online, *Figure S16*). Moreover, the whole-brain weight maps and the most predictive components also showed high similarities between participants taking or not taking antihypertensives (*Figure 5*; see Supplementary material online, *Figure S17 and Table S5*). Nevertheless, certain brain components contributed differentially to these two groups. Specifically, IC-18 (inferior parietal and postcentral gyrus), IC-36 (precuneus), and IC-37 (middle frontal gyrus) demonstrated greater predictive power for medicated than unmediated participants in predicting SBP, whereas, IC-31 (middle frontal gyrus), IC-49 (angular gyrus), and IC-18 contributed more to medicated than unmediated participants in predicting DBP.

4. Discussion

In this study, using the largest imaging sample currently available, we delineate BP-related brain signatures using whole-brain connectomes and machine learning with relatively high effect sizes and robust

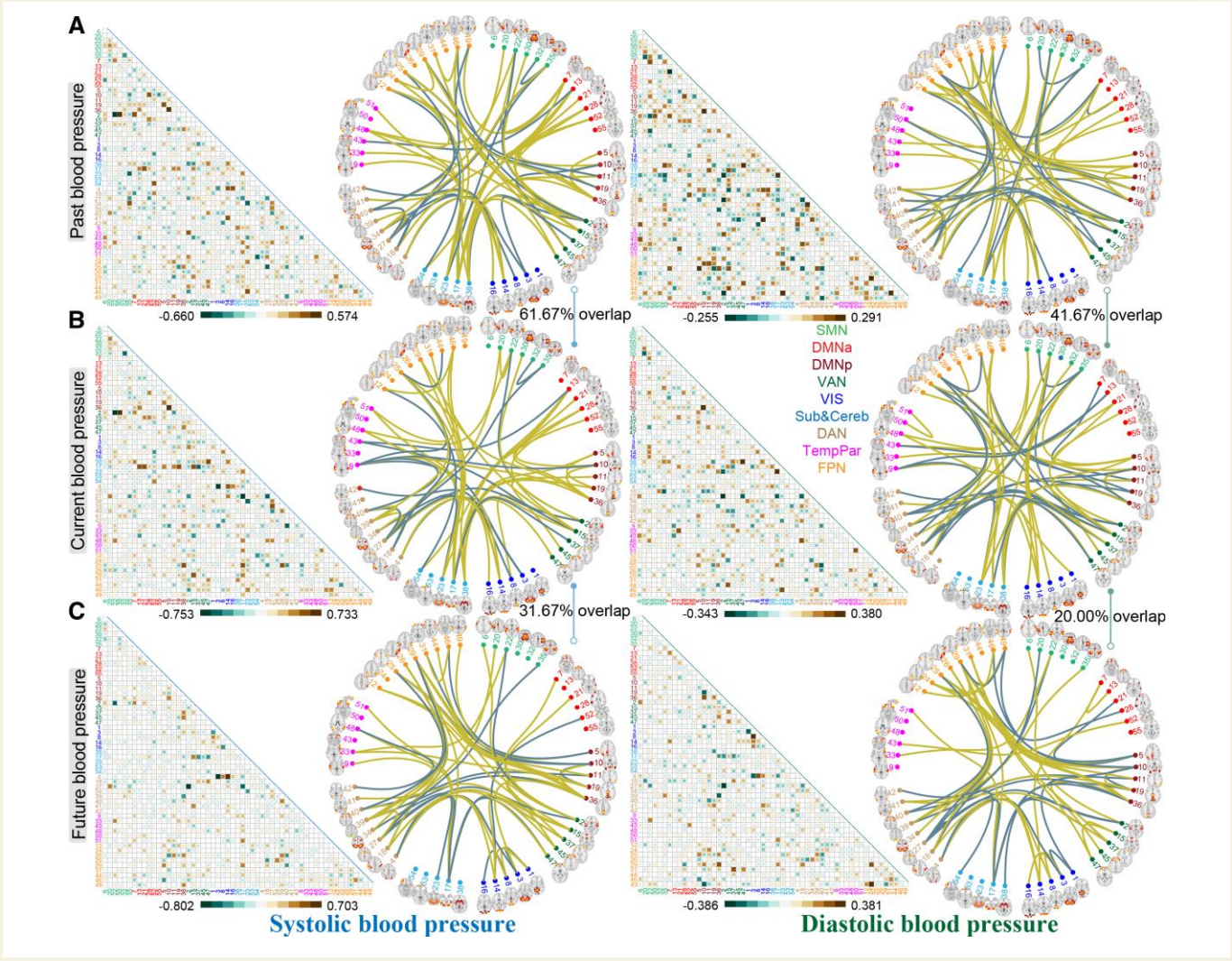

Figure 3 Distributions of predictive weights and the most predictive connections. Cell plots depict the raw weights map averaged across 200 cross-validation loops in predicting (*A*) previous, (*B*) current and (*C*) future SBP/DBP. Circle plots illustrate the top 60 edges having the highest predictive contributions. Among the top 60 edges, the SBP-current model shared 61.67% connections with the SBP-past model, and 31.67% connections with the SBP-future model, while, the DBP-current model had 41.67 and 20% connections in common with DBP-past and DBP-future models. Similar visualizations for PP can be found in Supplementary material online, *Figure S11*.

generalizability. Our identified brain signatures show prominent connectivity patterns among cerebellum, PFC, anterior insula, ACC, supramarginal gyrus, and precuneus, which are key regions of the central autonomic network, and involved in cognition processing and susceptible to neurodegeneration in AD.[40] Moreover, we revealed overlapping and distinct brain patterns in predicting BP levels between participants on and off antihypertensive medication (*Figure 6*). Taken together, we identify neural signatures underlying BP, providing evidence for meaningful BP-associated neural representations in connectivity profiles.

Our models provide evidence that BP involves a distributed set of neural processes. Among all predictors, the cerebellum demonstrates the highest contribution across all three time points, underscoring the importance of functional connectivity between the cerebellum and other brain regions in regulating BP. This finding is supported by experimental and epidemiological studies suggesting the existence of a cerebellar adrenomedullinergic system, which is crucial in body fluid homeostasis and BP regulation .[41] During hypertension, the adrenomedullin and its receptor components in the cerebellum would be altered. Oral administration of valsartan, on the other hand, can effectively reduce BP, and reverse the altered expression of adrenomedullin and its receptor components.[42] Moreover, one case report described a 60 mmHg rise in SBP and a fivefold increase in plasma noradrenaline following partial cerebellar resection for a 20-year-old man.[43] These findings, together with ours, suggested the crucial role of cerebellum plays in BP regulation.

Apart from the cerebellum, other brain regions whose connectivity patterns play a prominent role in explaining the success of BP-predictive models involve the anterior insula, ACC, PFC, supramarginal gyrus, and precuneus, which primarily implicate in functional networks of default model, salience, and FPNs. As a sympathetic regulatory centre, the insula is reported to have dense connections to autonomic nuclei via the brainstem and mesencephalon,[44] constituting

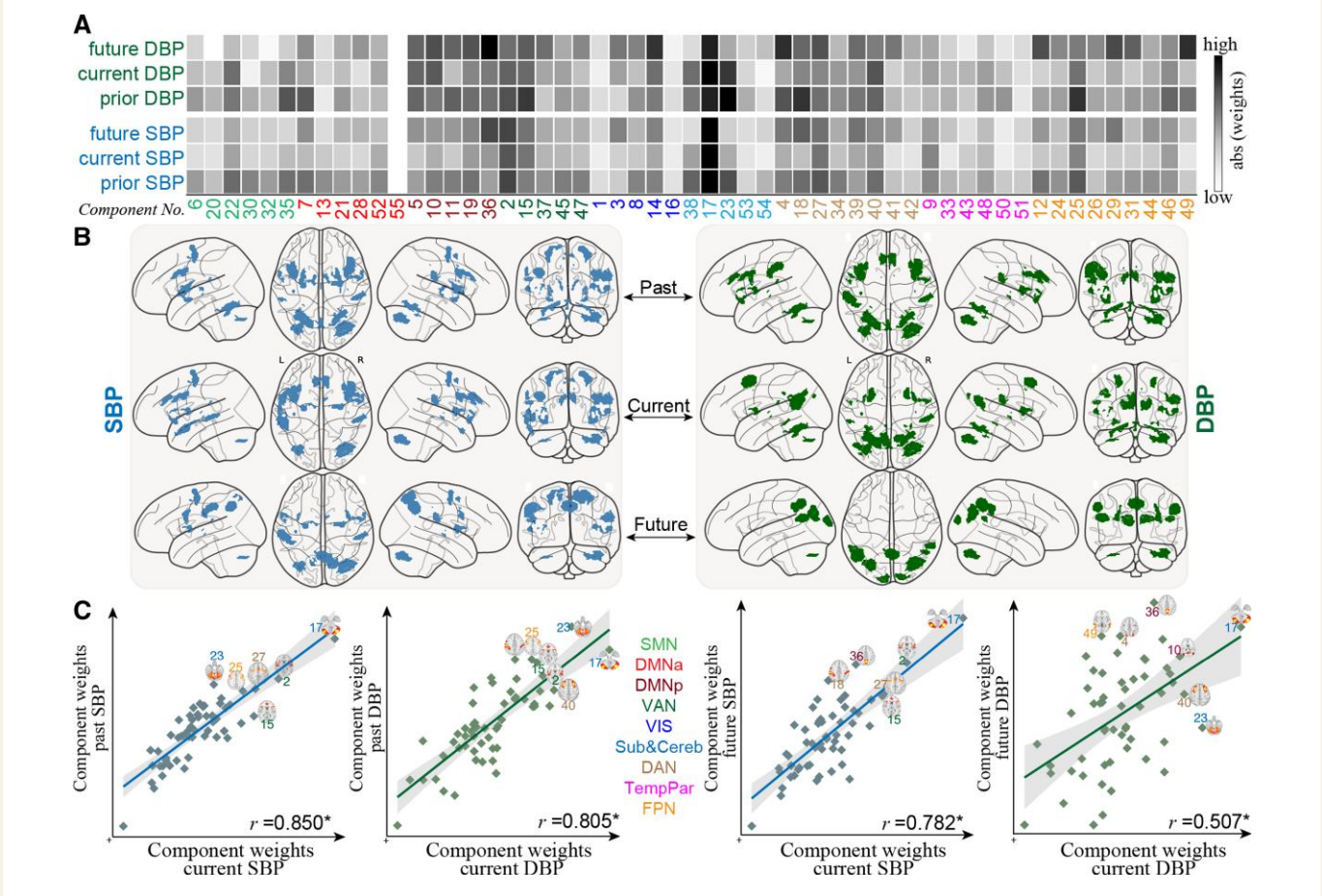

Figure 4 Functional neuroanatomical basis of the predictive brain signatures and the overlap between models from different time points. (*A*) Component-level representations of mean absolute weights in predicting past, current, and future SBP/DBP. Darker cell colors indicate greater predictive contribution. (*B*) For each model, the top six components with the highest predictive power are overlaid on a glass brain. (*C*) Correlations of component-level weight maps between SBP and DBP at each time point, as well as between different time points. DMNa, default mode network anterior; DMNp, default mode network posterior; SMN, somatomotor network; Sub&Cereb, subcortical and cerebellar network; TempPar, temporoparietal network; VAN, ventral attention network; VIS, visual network.

the primary site of viscerosensory integration and homeostasis modulation via baroafferents from amygdala and thalamus and afferents to brainstem.[45] Supporting the role of insula in BP regulation, a recent fMRI study found that intrinsic connectivity between insula and midbrain-brainstem-cerebellar network could be used to differentiate hypertensives from normotensives.[46] Also supportive of our results was the demonstration that acupuncture treatment increased functional connectivity between hypothalamus and brainstem, cerebellum, insula, ACC, and PFC.[47,48] Moreover, lesion studies revealed that damages to the left insula in stroke were associated with elevated SBP.[49] Consistently, Feng *et al.*[15] also found that connectivity patterns of hippocampal and PFC were linked to a history of hypertension, and mediated its relationship with cognition function.

Moreover, some studies suggested a network overlap between patients with hypertension and depression. Specifically, Maaike *et al.*[50] identified a set of brain regions including cerebellum, insula, ACC, and PFC that exhibit overlapping abnormalities in depression and hypertension, possibly due to the shared risk factor of stress. These results may suggest the involvement of these functional regions in emotional and cognitive processing, as well as autonomic modulation.

A recent review[51] identified 23 regions commonly associated with both cardiovascular risk factors (hypertension and Type 2 diabetes) and Alzheimer's dementia. Interestingly, all brain components identified from our prediction analysis were included in these 23 regions. These results imply a potential pathophysiologic link between hypertension and AD. Specifically, according to the two-hit vascular hypothesis of AD, cardiovascular risk factors including hypertension first impact the cerebral blood flow and blood-brain barrier, followed by an increase in beta-amyloid accumulation, resulting in neurodegeneration and diseases.[52,53] Consequently, it is speculated that BP-related brain damage may occur predominantly in functional networks targeted by AD pathology, which include DMN, FPN and the salience network. These functional networks are important sites of pathology accumulation in AD and are more susceptible to vascular risk burdens.[13] Specifically, the DMN and FPN participate in a series of high-order cognitive tasks, and thus have the highest metabolic demands, rendering them particularly vulnerable to neurovascular damages.[25,54] The reductions in cerebrovascular reactivity,[55] cerebral blood flow,[56] and metabolism[57] following elevated BP may disrupt the internal balance and integrity of DMN and FPN. Growing evidence implies that changes in brain

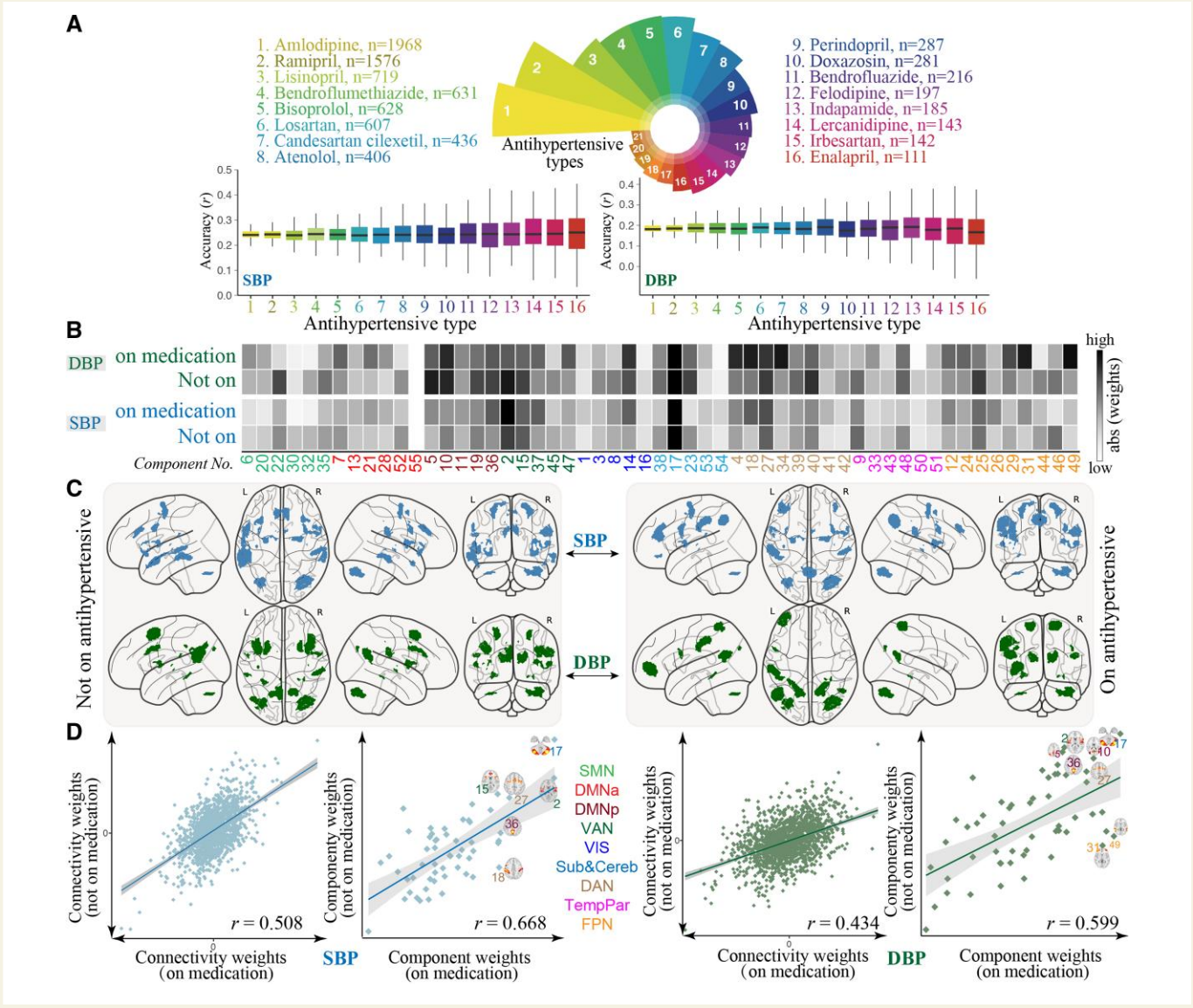

Figure 5 Functional neuroanatomical basis of the predictive brain signatures for participants on or off antihypertensive medication. (*A*). Distributions of prediction accuracies on participants grouped by the type of antihypertensive treatment. These results were only reported for antihypertensive medications taken by more than 100 patients. (*B*) Component-level representations of mean absolute weights in predicting SBP/DBP. Darker cell colors indicate greater predictive contribution. (*C*) For each model, the top 6 components with the highest predictive power are overlaid on a glass brain. (*D*) Correlations of edge- and component-level weight maps between participants on or off BP-lowering medication for SBP/DBP. SBP, DMNa, default mode network anterior; DMNp, default mode network posterior; SMN, somatomotor network; Sub&Cereb, subcortical and cerebellar network; TempPar, temporoparietal network; VAN, ventral attention network; VIS, visual network.

connectomes of DMN and FPN have a close affinity to the development of cognitive impairment.[24,55,58] In this regard, we speculated the involvement of more DMN and FPN regions in predicting future BP may indicate that they act as a compensatory mechanism to allow better preservation of cognitive functions,[24] when vascular damages are more evident and cognitive dysfunctions are severe. This may also account for the more involvement of these networks in medicated participants, since taking mediation per se implies a longer exposure to hypertension and a greater degree of cognitive impairment.

While we interpret our models based on neural functions, an alternative explanation is that these signatures represent individual differences in hemodynamics. For example, the cerebellum is irrorated from the basilar artery, while the cortex is mainly irrorated from vessels downstream of the Willis' circle. Individual differences in BP levels may be associated with individual differences in hemodynamics between these regions, which could then lead to changes in functional connectivity that do not reflect individual differences in neural functioning. Unfortunately, with only resting-state fMRI data, it is not possible to distinguish between these two explanations. Thus, caution is warranted for the interpretations above. Indeed, a combination of neural and hemodynamic factors likely best explains our observed connectivity patterns.

This work builds upon a spate of research documenting the associations of BP levels with multimodal brain MRI indices,[4,6,24,40,59] and extends them in several ways. First, prior studies in cardiovascular risk

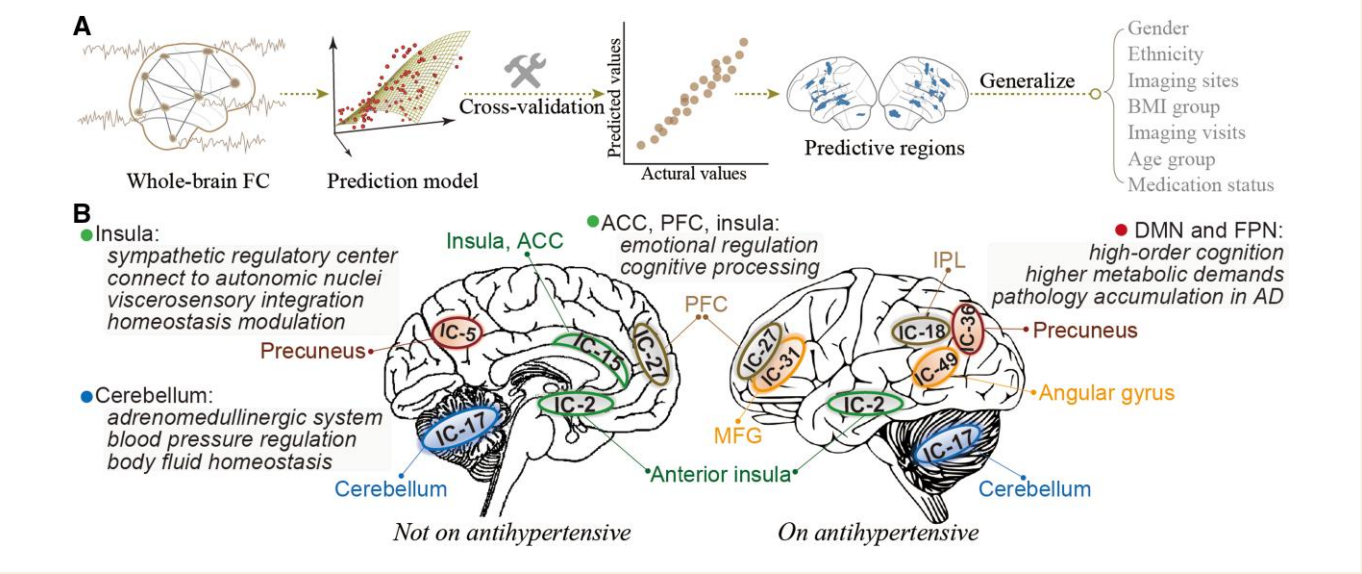

Figure 6 Summary of the analytical procedure and key predictive brain regions of BP values. (*A*) Within a 10-fold cross-validation framework, we implemented a data-driven, machine learning approach to predict individuals' BP levels based on whole-brain connectomes, and then examined the generalizability across multiple contexts. (*B*) The predictive models identified a set of brain regions including the cerebellum, PFC, anterior insula, ACC, supramarginal gyrus, and precuneus, which are key regions of the central autonomic network, and involved in cognition processing and susceptible to neurodegeneration in AD. The DMN and FPN revealed more involvement in participants taking antihypertensive medication. ACC, anterior cingulate cortex; DMN, default mode network; FC, functional connectivity; IC, independent component; PFC, prefrontal cortex.

factors including hypertension have been predominantly informed by brain structure, with a particular emphasis on WMH.[60] In comparison, we leveraged functional connectivity, which is based on the mechanism of neurovascular coupling to quantify neural communications among brain regions, to delineate the neurobiological correlates of BP. This is motivated by increasing neuroimaging evidence that resting-state functional connectivity is more sensitive to subtle abnormalities related to aging and brain diseases,[13,14] and more importantly, changes in brain function appear earlier than structural alterations.[11,61] As such, it may take years for BP-related changes to become evident and detectable in brain structure, supporting the finding that the past instead of current vascular risk factor burden is a superior predictor of brain volume[10] and WMH.[7] In contrast, we revealed comparable prediction accuracies for current and past BP, which can be attributed to the high sensitivity of functional connectome in detecting brain-phenotype relationships. Promisingly, our current use of functional connectivity may afford us more opportunities to identify early biomarkers related to elevated BP.

Second, previous studies primarily focused on detecting brain features that either significantly differ between hypertensives and controls, or correlate with BP values. For example, based on the same UK Biobank cohort, Feng *et al.*[15] identified a set of functional links that significantly differ between participants with a history of hypertension and those without. In contrast we attempted to identify a brain signature capable of accurately predicting BP level from an individual's unique connectivity profiles, which places the implications of current findings in a quantitative perspective. Further, instead of focusing on current BP levels, we also examined the predictability of past and future BP levels from brain connectivity, which has never been examined by other studies.[15] Indeed, recent studies have also shown that BP-related brain changes occur in an ongoing manner,[6] and can commence approximately ten years before clinically evident symptoms of hypertension,[56] during which brain injury and cognitive decline are no longer reversible.

Third, the large sample size is a prominent strength. Previous investigations examining brain-BP associations have generally been small or moderate, which significantly limited the strength of inferences. In comparison, the current use of the large sample of population-based participants enables the identification of subtle effects that may not be statistically detectable in smaller groups, as well as the establishment of reliable estimates of neurobiological correlates of BP.[29,62] Additionally, the multivariate nature of machine learning approaches enables us to account adequately for the regional heterogeneity in BP-related brain changes by aggregating the weak effects of individual brain connections into an integrated brain index, which has a large effect size.

Fourth, the BP-predictive brain signatures showed strong generalizability across contexts, corroborating our model's robustness in capturing reliable brain-BP relationships rather than sample-specific idiosyncrasies.[16,21] The identification of this brain signature may potentially (i) increase confidence in using the developed model to identify sensitive neuromarkers of elevated BP at an early stage related diseases and (ii) facilitate targeted therapies to preserve brain function and prevent cognitive decline in late life,[63] although more clinical trials are needed. Further, among all potential covariates, we found age has the greatest impact on the prediction of SBP but minimal impact on DBP. This could be attributable to the temporally distinct trajectories of SBP and DBP. This hypothesis gains support from recent evidence that SBP increased linearly with age, while DBP showed a nonlinear aging trajectory.[60,64] Consistently, additional analysis in our data revealed a similar result (see Supplementary material online, *Figure S18*). These findings necessitate future examination of the intricate interplay and combined effects of multiple cardiovascular risk factors on brain structure and function.[36]

Overall, our study provided an imaging-based brain signature for BP at the individual level. The use of functional connectivity may afford us

more opportunities to identify early biomarkers to improve prevention and diagnosis of hypertension prior to the clinical onset of overt symptoms. Moreover, the current practice of predicting BP value on a continuum spanning from health to disorder, rather than the simple presence or absence of hypertension, opens a promising window for monitoring the progression of brain alterations associated with BP, which accords with the concept of personalized treatment in precision medicine.[65] In addition, the findings represent a critical step in informing our understanding of the associations between BP and brain function. The identified imaging signatures may also serve as a target for novel therapeutics, especially given the absence of prior evidence showing the beneficial effects of BP-lowering on cardiovascular diseases and cognitive deficits.[66,67]

Notwithstanding strengths in terms of large sample size and multiple validations, several limitations should be acknowledged. First, the cross-sectional nature of our current analysis does not allow disentangling the causality between BP and brain signatures identified here. That is, we cannot make any conclusions about whether the identified brain connectivity induces elevated BP, or is simply a result of elevated BP. As more data are being acquired by UK Biobank sequentially, longitudinal progression of BP-related brain indices merits further inquiry. Second, the interval between the first and repeated imaging visits was relatively short. Consequently, the extent to which the constructed models can be applied to predict BP levels with a longer follow-up remains to be determined in future studies. Further, in light of the short time interval, it is possible that the predictability of future BP levels may be driven by the high correlations of BP values between the two imaging visits. Our additional analyses indicated that predictions for participants with stable BP values across time were more accurate than those showing variable BP levels, yet predictions in both groups were significant (see Supplementary material online, *Figure S19*). However, the weight maps between these two groups were highly similar, suggesting that the predictive models identified reliable brain signatures underlying individual differences in BP levels. In subsequent waves of UK Biobank data, studies should further examine the predictability of future BP values with greater variability. Third, although we highlighted and discussed a set of brain regions that may play important roles in the regulation of BP levels, it should be noted that it was not the pattern activity of these regions that contributed to the prediction, but their functional connectivity with other regions. Our further analyses suggested that the component amplitudes and functional connectivity may contain overlapping information that is crucial for BP prediction (see Supplementary material online, *Figure S20 and S21*). Specifically, we found that the components whose amplitude showed the highest correlation with BP levels were largely overlapped with those showing the highest predictive weights, suggesting that activity amplitude and connectivity patterns may be highly correlated. Forth, participants in the UK Biobank cohort have lower death rates and show a proclivity to live in less deprived areas,[2] potentially limiting the predictive model's generalizability. Nevertheless, this may not be a problem in light of our control analysis demonstrating a negligible effect of socioeconomic status on predictions. Fifth, the prediction accuracy was relatively low after controlling for numerous covariates, and thus, there is still plenty of room for improving. Sixth, although the use of UK Biobank data enables us to investigate the impact of a large range of potential confounders, it is possible that some unrecognized confounders may affect the results. Finally, cognitive data were not analyzed in this study. Further studies can elaborate on how functional network patterns mediate the association between BP and core cognitive abilities.[24]

5. Summary

In sum, we developed, based on the largest sample currently available, a robust and generalizable connectome-based brain signature that is able to predict individuals' past, current, and future BP levels. We revealed a set of brain regions whose connectivity patterns underlie BP regulation including cerebellum, insula, ACC, supramarginal gyrus, and PFC. Overall, our current study sheds light on how individual differences in BP are represented in the brain connectivity patterns, and may promisingly facilitate the identification of biomarkers to preserve brain function and prevent cognitive decline.

Supplementary material

Supplementary material is available at *Cardiovascular Research* online.

Authors' contributions

R.J. and D.S. conceived and designed the experiment. R.J. performed the analyses with support from D.S., J.S., and S.N. R.J. and D.S. wrote the paper with contributions from S.N., V.C. and comments from all other authors.

Acknowledgements

This research was conducted using the UK Biobank resource under application number34 175. We are grateful to all participants who donated their time to this project and the UK Biobank team for collecting, processing, and disseminating data used in this study.

Conflict of interest: None declared.

Funding

This work was supported by the National Institute of Mental Health [K00MH122372]; the National Institutes of Health [RF1AG063153]; and the National Science Foundation [2112455].

Data availability

All data used in this study are publicly accessible from UK Biobank via their standard data access procedure at https://www.ukbiobank.acuk/. Code used in the current study is available from the authors upon request.

References

1. Wan EYF, Fung WT, Schooling CM, Au Yeung SL, Kwok MK, Yu EYT, Wang Y, Chan EWY, Wong ICK, Lam CLK. Blood pressure and risk of cardiovascular disease in UK biobank: a Mendelian randomization study. *Hypertension* 2021;**77**:367–375.
2. Littlejohns TJ, Sudlow C, Allen NE, Collins R. UK Biobank: opportunities for cardiovascular research. *Eur Heart J* 2019;**40**:1158–1166.
3. Iadecola C, Gottesman RF. Neurovascular and cognitive dysfunction in hypertension. *Circ Res* 2019;**124**:1025–1044.
4. Carnevale L, D'Angelosante V, Landolfi A, Grillea G, Selvetella G, Storto M, Lembo G, Carnevale D. Brain MRI fiber-tracking reveals white matter alterations in hypertensive patients without damage at conventional neuroimaging. *Cardiovasc Res* 2018;**114**:1536–1546.
5. Cox SR, Lyall DM, Ritchie SJ, Bastin ME, Harris MA, Buchanan CR, Fawns-Ritchie C, Barbu MC, De Nooij L, Reus LM, Alloza C, Shen XY, Neilson E, Alderson HL, Hunter S, Liewald DC, Whalley HC, McIntosh AM, Lawrie SM, Pell JP, Tucker-Drob EM, Wardlaw JM, Gale CR, Deary IJ. Associations between vascular risk factors and brain MRI indices in UK biobank. *Eur Heart J* 2019;**40**:2290–2300.
6. Schaare HL, Kharabian Masouleh S, Beyer F, Kumral D, Uhlig M, Reinelt JD, Reiter AMF, Lampe L, Babayan A, Erbey M, Roebbig J, Schroeter ML, Okon-Singer H, Muller K, Mendes N, Margulies DS, Witte AV, Gaebler M, Villringer A. Association of peripheral

blood pressure with gray matter volume in 19- to 40-year-old adults. *Neurology* 2019;**92**:e758–e773.
7. Wartolowska KA, Webb AJS. Midlife blood pressure is associated with the severity of white matter hyperintensities: analysis of the UK biobank cohort study. *Eur Heart J* 2021;**42**:750–757.
8. Lane CA, Barnes J, Nicholas JM, Sudre CH, Cash DM, Parker TD, Malone IB, Lu K, James S-N, Keshavan A, Murray-Smith H, Wong A, Buchanan SM, Keuss SE, Gordon E, Coath W, Barnes A, Dickson J, Modat M, Thomas D, Crutch SJ, Hardy R, Richards M, Fox NC, Schott JM. Associations between blood pressure across adulthood and late-life brain structure and pathology in the neuroscience substudy of the 1946 British birth cohort (insight 46): an epidemiological study. *Lancet Neurol* 2019;**18**:942–952.
9. Maillard P, Seshadri S, Beiser A, Himali JJ, Au R, Fletcher E, Carmichael O, Wolf PA, DeCarli C. Effects of systolic blood pressure on white-matter integrity in young adults in the framingham heart study: a cross-sectional study. *Lancet Neurol* 2012;**11**:1039–1047.
10. Pase MP, Davis-Plourde K, Himali JJ, Satizabal CL, Aparicio H, Seshadri S, Beiser AS, DeCarli C. Vascular risk at younger ages most strongly associates with current and future brain volume. *Neurology* 2018;**91**:1479–1486.
11. Gonneaud J, Baria AT, Pichet Binette A, Gordon BA, Chhatwal JP, Cruchaga C, Jucker M, Levin J, Salloway S, Farlow M, Gauthier S, Benzinger TLS, Morris JC, Bateman RJ, Breitner JCS, Poirier J, Vachon-Presseau E, Villeneuve S, Alzheimer's Disease Neuroimaging Initiative (ADNI); Dominantly Inherited Alzheimer Network (DIAN) Study Group; Pre-symptomatic Evaluation of Experimental or Novel Treatments for Alzheimer's Disease (PREVENT-AD) Research Group. Accelerated functional brain aging in pre-clinical familial Alzheimer's disease. *Nat Commun* 2021;**12**:5346.
12. Than S, Srikanth V. Detecting brain injury related to hypertension at mid-life: a key to interventions for preventing dementia in older age. *Cardiovasc Res* 2018;**114**:1430–1431.
13. Zonneveld HI, Pruim RH, Bos D, Vrooman HA, Muetzel RL, Hofman A, Rombouts SA, van der Lugt A, Niessen WJ, Ikram MA, Vernooij MW. Patterns of functional connectivity in an aging population: the rotterdam study. *Neuroimage* 2019;**189**:432–444.
14. Haight TJ, Bryan RN, Erus G, Davatzikos C, Jacobs DR, D'Esposito M, Lewis CE, Launer LJ. Vascular risk factors, cerebrovascular reactivity, and the default-mode brain network. *Neuroimage* 2015;**115**:7–16.
15. Feng RQ, Rolls ET, Cheng W, Feng JF. Hypertension is associated with reduced hippocampal connectivity and impaired memory. *Ebiomedicine* 2020;**61**:103082.
16. Sui J, Jiang R, Bustillo J, Calhoun V. Neuroimaging-based individualized prediction of cognition and behavior for mental disorders and health: methods and promises. *Biol Psychiatry* 2020;**88**:818–828.
17. Poldrack RA, Huckins G, Varoquaux G. Establishment of best practices for evidence for prediction: a review. *JAMA Psychiat* 2020;**77**:534–540.
18. Rosenberg MD, Finn ES, Scheinost D, Papademetris X, Shen X, Constable RT, Chun MM. A neuromarker of sustained attention from whole-brain functional connectivity. *Nat Neurosci* 2016;**19**:165–171.
19. Woo CW, Chang LJ, Lindquist MA, Wager TD. Building better biomarkers: brain models in translational neuroimaging. *Nat Neurosci* 2017;**20**:365–377.
20. Lee JJ, Kim HJ, Čeko M, Park BY, Lee SA, Park H, Roy M, Kim SG, Wager TD, Woo CW. A neuroimaging biomarker for sustained experimental and clinical pain. *Nat Med* 2021;**27**:174–182.
21. Scheinost D, Noble S, Horien C, Greene AS, Lake EM, Salehi M, Gao S, Shen X, O'Connor D, Barron DS, Yip SW, Rosenberg MD, Constable RT. Ten simple rules for predictive modeling of individual differences in neuroimaging. *Neuroimage* 2019;**193**:35–45.
22. Miller KL, Alfaro-Almagro F, Bangerter NK, Thomas DL, Yacoub E, Xu J, Bartsch AJ, Jbabdi S, Sotiropoulos SN, Andersson JL, Griffanti L, Douaud G, Okell TW, Weale P, Dragonu I, Garratt S, Hudson S, Collins R, Jenkinson M, Matthews PM, Smith SM. Multimodal population brain imaging in the UK biobank prospective epidemiological study. *Nat Neurosci* 2016;**19**:1523–1536.
23. Bycroft C, Freeman C, Petkova D, Band G, Elliott LT, Sharp K, Motyer A, Vukcevic D, Delaneau O, O'Connell J, Cortes A, Welsh S, Young A, Effingham M, McVean G, Leslie S, Allen N, Donnelly P, Marchini J. The UK biobank resource with deep phenotyping and genomic data. *Nature* 2018;**562**:203–209.
24. Jenkins LM, Kogan A, Malinab M, Ingo C, Sedaghat S, Bryan NR, Yaffe K, Parrish TB, Nemeth AJ, Lloyd-Jones DM, Launer LJ, Wang L, Sorond F. Blood pressure, executive function, and network connectivity in middle-aged adults at risk of dementia in late life. *Proc Natl Acad Sci U S A* 2021;**118**:e2024265118.
25. Kobe T, Binette AP, Vogel JW, Meyer PF, Breitner JCS, Poirier J, Villeneuve S, Presymptomatic Evaluation of Novel or Experimental Treatments for Alzheimer Disease (PREVENT-AD) Research Group. Vascular risk factors and functional connectivity changes. *Neuroimage* 2021;**231**:117832.
26. Mancia G, Grassi G. The autonomic nervous system and hypertension. *Circ Res* 2014;**114**:1804–1814.
27. Neitzel J, Malik R, Muetzel R, Knol MJ, Zonneveld H, Georgakis MK, Franzmeier N, Rubinski A, Dichgans M, Ikram MA. Genetic variants link lower segregation of brain networks to higher blood pressure and worse cognition within the general aging population. *medRxiv* 2021. doi:10.1101/2021.08.12.21261975.
28. Alfaro-Almagro F, Jenkinson M, Bangerter NK, Andersson JLR, Griffanti L, Douaud G, Sotiropoulos SN, Jbabdi S, Hernandez-Fernandez M, Vallee E, Vidaurre D, Webster M, McCarthy P, Rorden C, Daducci A, Alexander DC, Zhang H, Dragonu I, Matthews PM, Miller KL, Smith SM. Image processing and quality control for the first 10,000 brain imaging datasets from UK biobank. *Neuroimage* 2018;**166**:400–424.
29. Maglanoc LA, Kaufmann T, van der Meer D, Marquand AF, Wolfers T, Jonassen R, Hilland E, Andreassen OA, Landro NI, Westlye LT. Brain connectome mapping of complex human traits and their polygenic architecture using machine learning. *Biol Psychiatry* 2020;**87**:717–726.
30. Krishnan A, Williams LJ, McIntosh AR, Abdi H. Partial least squares (PLS) methods for neuroimaging: a tutorial and review. *Neuroimage* 2011;**56**:455–475.
31. Hyon R, Youm Y, Kim J, Chey J, Kwak S, Parkinson C. Similarity in functional brain connectivity at rest predicts interpersonal closeness in the social network of an entire village. *Proc Natl Acad Sci U S A* 2020;**117**:33149–33160.
32. Jiang R, Zuo N, Ford JM, Qi S, Zhi D, Zhuo C, Xu Y, Fu Z, Bustillo J, Turner JA. Task-induced brain connectivity promotes the detection of individual differences in brain-behavior relationships. *NeuroImage* 2020;**207**:116370.
33. Yoo K, Rosenberg MD, Hsu WT, Zhang S, Li CR, Scheinost D, Constable RT, Chun MM. Connectome-based predictive modeling of attention: comparing different functional connectivity features and prediction methods across datasets. *Neuroimage* 2018;**167**:11–22.
34. Cui Z, Li H, Xia CH, Larsen B, Adebimpe A, Baum GL, Cieslak M, Gur RE, Gur RC, Moore TM, Oathes DJ, Alexander-Bloch AF, Raznahan A, Roalf DR, Shinohara RT, Wolf DH, Davatzikos C, Bassett DS, Fair DA, Fan Y, Satterthwaite TD. Individual variation in functional topography of association networks in youth. *Neuron* 2020;**106**:340–353.e348.
35. Ferguson AC, Tank R, Lyall LM, Ward J, Welsh P, Celis-Morales C, McQueenie R, Strawbridge RJ, Mackay DF, Pell JP, Smith DJ, Sattar N, Cavanagh J, Lyall DM. Association of SBP and BMI with cognitive and structural brain phenotypes in UK biobank. *J Hypertens* 2020;**38**:2482–2489.
36. Veldsman M, Tai XY, Nichols T, Smith S, Peixoto J, Manohar S, Husain M. Cerebrovascular risk factors impact frontoparietal network integrity and executive function in healthy ageing. *Nat Commun* 2020; **11**:4340.
37. Sripada C, Rutherford S, Angstadt M, Thompson WK, Luciana M, Weigard A, Hyde LH, Heitzeg M. Prediction of neurocognition in youth from resting state fMRI. *Mol Psychiatry* 2020;**25**:3413–3421.
38. Dosenbach NU, Nardos B, Cohen AL, Fair DA, Power JD, Church JA, Nelson SM, Wig GS, Vogel AC, Lessov-Schlaggar CN. Prediction of individual brain maturity using fMRI. *Science* 2010;**329**:1358–1361.
39. Jiang R, Calhoun VD, Fan L, Zuo N, Jung R, Qi S, Lin D, Li J, Zhuo C, Song M, Fu Z, Jiang T, Sui J. Gender differences in connectome-based predictions of individualized intelligence quotient and sub-domain scores. *Cereb Cortex* 2020;**30**:888–900.
40. Beauchet O, Celle S, Roche F, Bartha R, Montero-Odasso M, Allali G, Annweiler C. Blood pressure levels and brain volume reduction: a systematic review and meta-analysis. *J Hypertens* 2013;**31**:1502–1516.
41. Figueira L, Israel A. Role of cerebellar adrenomedullin in blood pressure regulation. *Neuropeptides* 2015;**54**:59–66.
42. Figueira L, Israel A. Effect of valsartan on cerebellar adrenomedullin system dysregulation during hypertension. *Cerebellum* 2017;**16**:132–141.
43. Idiaquez J, Fadic R, Mathias CJ. Transient orthostatic hypertension after partial cerebellar resection. *Clin Auton Res* 2011;**21**:57–59.
44. Gianaros PJ, Onyewuenyi IC, Sheu LK, Christie IC, Critchley HD. Brain systems for baroreflex suppression during stress in humans. *Hum Brain Mapp* 2012;**33**:1700–1716.
45. Critchley HD, Harrison NA. Visceral influences on brain and behavior. *Neuron* 2013;**77**:624–638.
46. McIntosh RC, Lobo JD, Yang A, Schneiderman N. Brainstem network connectivity with mid-anterior insula predicts lower systolic blood pressure at rest in older adults with hypertension. *J Hum Hypertens* 2021;**35**:1098–1108.
47. Chen H, Dai J, Zhang X, Wang K, Huang S, Cao Q, Wang H, Liang Y, Shi C, Li M, Ha T, Ai L, Li S, Ma J, Wei W, You Y, Liu Z, Tian J, Bai L. Hypothalamus-related resting brain network underlying short-term acupuncture treatment in primary hypertension. *Evid Based Complement Alternat Med* 2013;**2013**:808971.
48. Zheng Y, Zhang J, Wang Y, Wang Y, Lan Y, Qu S, Tang C, Huang Y. Acupuncture decreases blood pressure related to hypothalamus functional connectivity with frontal lobe, cerebellum, and insula: A study of instantaneous and short-term acupuncture treatment in essential hypertension. *Evid Based Complement Alternat Med* 2016;**2016**:6908710.
49. Inamasu J, Sugimoto K, Watanabe E, Kato Y, Hirose Y. Effect of insular injury on autonomic functions in patients with ruptured middle cerebral artery aneurysms. *Stroke* 2013;**44**:3550–3552.
50. Meurs M, Groenewold NA, Roest AM, van der Wee NJ, Veltman DJ, van Tol MJ, de Jonge P. The associations of depression and hypertension with brain volumes: independent or interactive? *Neuroimage Clin* 2015;**8**:79–86.
51. Lamar M, Boots EA, Arfanakis K, Barnes LL, Schneider JA. Common brain structural alterations associated with cardiovascular disease risk factors and Alzheimer's dementia: future directions and implications. *Neuropsychol Rev* 2020;**30**:546–557.
52. Zlokovic BV. Neurovascular pathways to neurodegeneration in Alzheimer's disease and other disorders. *Nat Rev Neurosci* 2011;**12**:723–738.
53. Tzourio C, Laurent S, Debette S. Is hypertension associated with an accelerated aging of the brain? *Hypertension* 2014;**63**:894–903.
54. Rashid B, Dev SI, Esterman M, Schwarz NF, Ferland T, Fortenbaugh FC, Milberg WP, McGlinchey RE, Salat DH, Leritz EC. Aberrant patterns of default-mode network

functional connectivity associated with metabolic syndrome: A resting-state study. *Brain Behav* 2019;**9**:e01333.
55. Lowry E, Puthusseryppady V, Johnen A-K, Renoult L, Hornberger M. Cognitive and neuroimaging markers for preclinical vascular cognitive impairment. *Cerebral Circulation-Cognition and Behavi* 2021;**2**:100029.
56. Jennings JR, Muldoon MF, Ryan C, Gach HM, Heim A, Sheu LK, Gianaros PJ. Prehypertensive blood pressures and regional cerebral blood flow independently relate to cognitive performance in midlife. *J Am Heart Assoc* 2017;**6**:e004856.
57. Kuczynski B, Jagust W, Chui HC, Reed B. An inverse association of cardiovascular risk and frontal lobe glucose metabolism. *Neurology* 2009;**72**:738–743.
58. Chen X, Huang LL, Ye Q, Yang D, Qin RM, Luo CM, Li MC, Zhang B, Xu Y. Disrupted functional and structural connectivity within default mode network contribute to WMH-related cognitive impairment. *Neuroimage Clin* 2019;**24**:102088.
59. Cox SR, Lyall DM, Ritchie SJ, Bastin ME, Harris MA, Buchanan CR, Fawns-Ritchie C, Barbu MC, De Nooij L, Reus LM, Alloza C, Shen X, Neilson E, Alderson HL, Hunter S, Liewald DC, Whalley HC, McIntosh AM, Lawrie SM, Pell JP, Tucker-Drob EM, Wardlaw JM, Gale CR, Deary IJ. Associations between vascular risk factors and brain MRI indices in UK biobank. *Eur Heart J* 2019;**40**:2290–2300.
60. Wilkinson I, Webb AJS. Consistency of associations of systolic and diastolic blood pressure with white matter hyperintensities: A meta-analysis. *Int J Stroke* 2021;**17**:291–298.
61. Jack CR J, Knopman DS, Jagust WJ, Shaw LM, Aisen PS, Weiner MW, Petersen RC, Trojanowski JQ. Hypothetical model of dynamic biomarkers of the Alzheimer's pathological cascade. *Lancet Neurol* 2010;**9**:119–128.
62. Westlye LT, Alnaes D, van der Meer D, Kaufmann T, Andreassen OA. Population-based mapping of polygenic risk for schizophrenia on the human brain: new opportunities to capture the dimensional aspects of severe mental disorders. *Biol Psychiatry* 2019;**86**:499–501.
63. Jenkins LM, Garner CR, Kurian S, Higgins JP, Parrish TB, Sedaghat S, Nemeth AJ, Lloyd-Jones DM, Launer LJ, Hausdorff JM, Wang L, Sorond FA. Cumulative blood pressure exposure, basal ganglia, and thalamic morphology in midlife. *Hypertension* 2020;**75**:1289–1295.
64. Webb AJS. Progression of arterial stiffness is associated with midlife diastolic blood pressure and transition to late-life hypertensive phenotypes. *J Am Heart Assoc* 2020;**9**:e014547.
65. Jameson JL, Longo DL. Precision medicine–personalized, problematic, and promising. *N Engl J Med* 2015;**372**:2229–2234.
66. Higgins H, Mason AM, Larsson SC, Gill D, Langenberg C, Burgess S. Estimating the population benefits of blood pressure lowering: A wide-angled Mendelian randomization study in UK biobank. *J Am Heart Assoc* 2021;**10**:e021098.
67. Mcneil CJ, Myint PK, Sandu AL, Potter JF, Staff R, Whalley LJ, Murray AD. Increased diastolic blood pressure is associated with MRI biomarkers of dementia-related brain pathology in normative ageing. *Age Ageing* 2018;**47**:95–100.

Translational perspective

Using machine learning approach, this study predicted individual differences in blood pressure from whole-brain functional connectivity at the individual level. The identified brain signature, which primarily involves the cerebellum, prefrontal, anterior insula, anterior cingulate cortex, supramarginal gyrus, and precuneus, may afford us more opportunities to identify early biomarkers to improve prevention and diagnosis of hypertension prior to the clinical onset of overt symptoms. Moreover, the imaging signatures may also serve as a potential target for novel therapeutics, which can promisingly facilitate the preservation of brain function and cognitive function.